INTERNATIONAL JOURNAL OF CIRCUIT THEORY AND APPLICATIONS
Int. J. Circ. Theor. Appl. (2016)
Published online in Wiley Online Library (wileyonlinelibrary.com). DOI: 10.1002/cta.2189

Application of the modified IDA-PBC for shunt active power filters control

Federico M. Serra[1,*,†], Cristian H. De Angelo[2] and Daniel G. Forchetti[2]

[1]*Laboratorio de Control Automático (LCA), UNSL, Villa Mercedes, San Luis, Argentina*
[2]*Grupo de Electrónica Aplicada (GEA), UNRC, Río Cuarto, Córdoba, Argentina*

SUMMARY

The design of a passivity-based nonlinear controller for a shunt active power filter to be used for the compensation of harmonic currents consumed by nonlinear loads is presented in this paper. The main objective of designed controller is to inject the necessary compensation current into the system so that the grid current is sinusoidal and balanced, regardless of whether the grid voltage is unbalanced and/or distorted. The references for the compensation currents are obtained from applying the *pq* theory. The controller is designed on the basis of a modified interconnection and damping assignment technique, which allows solving a tracking control problem. An integral action controller is added to the proposed controller using the same design technique, in order to eliminate the errors produced by parameter variations or uncertainties. The behavior of the proposed control strategy is validated through simulation using a realistic model, which includes converter switching and losses, grid distortion, and parameter variations. Copyright © 2016 John Wiley & Sons, Ltd.

Received 19 January 2015; Revised 27 April 2015; Accepted 4 December 2015

KEY WORDS: shunt active power filter; interconnection and damping assignment; passivity-based control; IDA; SAPF

1. INTRODUCTION

The use of nonlinear loads has increased in last decades because of the progress in the development of power electronic devices. A load of this type consumes high harmonic currents, which must be supplied by the power source and transported by the transmission lines, producing additional losses because of the increase in the effective value of such currents. Besides producing losses in the transmission lines, consuming high harmonic currents reduces the quality of supplied energy and may undergo penalties. Therefore, avoiding harmonics and eliminating them imply a reduction in costs of the whole system operation.

In order to compensate harmonic currents, the use of shunt active power filter (SAPF) has been proposed [1–4]. Such power filters consist of a converter, a passive filter, and a controller, as schematized in Figure 1.

The converter used to implement the SAPF is a voltage source converter (VSC), with a resistor–inductor filter that allows the injection of the compensation currents into the power system.

Shunt active power filter must inject compensation currents with the appropriate waveform into the power system, so that currents supplied by the grid remain sinusoidal and balanced, regardless of the waveform of grid voltages. This implies a correct calculation of the compensating current references

*Correspondence to: Federico M. Serra, Facultad de Ingenieria y Ciencias Agropecuarias – Universidad Nacional de San Luis, Laboratorio de Control Automatico (LCA).
†E-mail: fserra@ieee.org

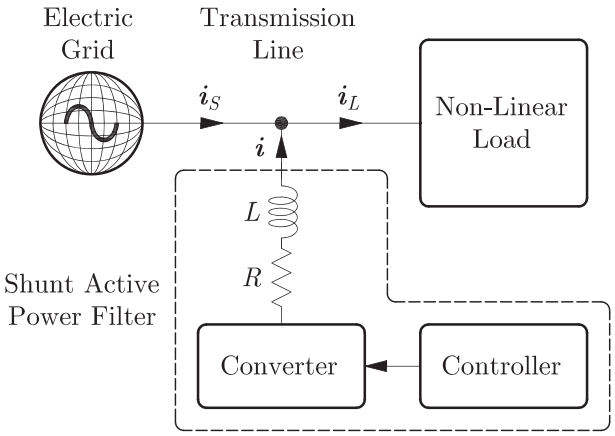

Figure 1. Compensation scheme with a shunt active power filter.

and a precise control of such currents. Moreover, controlling the VSC, direct current (DC) voltage is necessary in order to ensure that the converter is capable of injecting the compensating currents [5, 6].

The appropriate compensating currents can be obtained from different approaches [1,7]. One of the most used techniques is based on the instantaneous active-reactive power theory, also known as *pq theory*, which allows calculating the reference currents from the real and imaginary powers defined by the control strategy [8].

Controlling the SAPF for injecting the compensating currents usually requires control algorithms with a good steady-state performance and high dynamic response. Some of the proposed strategies include adaptive control, internal model control, sliding mode control, and nonlinear auto-disturbance rejection control, among others [5,9].

Passivity-based control [10] is a control design technique that has been used satisfactorily in many electrical systems, such as electric machines [11–13], power systems [14, 15], and power electronic converters [16]. One of these methods is the so-called interconnection and damping assignment (IDA) [17, 18], which consists in modifying the system's energy function in order to obtain a desired closed-loop structure, allowing system stabilization in regulation problems. This technique has been previously used for designing control strategies in VSCs used as rectifiers and inverters [19, 20].

In many of these applications of VSC, control objective consists in regulation to a constant set point (e.g., a rectifier with constant DC output, or an inverter with constant voltage output in a synchronous reference frame). Thus, the controller can be designed using the IDA approach proposed in [17, 18]. However, controlling a SAPF implies a tracking control problem, with a variable reference, which depends on load and grid behavior. A similar problem occurs for control design of VSC working as rectifier with unity power factor. For such case, a generalized state space averaging approach has been proposed in [19] in order to transform the tracking problem into a regulation one, and then be able to use the classical IDA approach. In [21], an incremental storage function is proposed to achieve the control objective.

In the present paper, a control strategy for a SAPF is designed with the objective of making the current supplied by the grid be sinusoidal and balanced. SAPF reference currents are calculated based on the *pq* theory, while the controller is designed based on the modified IDA methodology proposed in [22].

A preliminary proposal of this control strategy was early presented by the authors in [23]. In this paper, the proposed strategy is derived based on the modified IDA methodology, which allows exploiting the advantages of IDA regarding structured design and stability guarantee and applying them to the problem of trajectory tracking of SAPF.

In addition, a nonlinear integral controller is proposed to reduce the error produced by parameter variations and uncertainties. Such integral controller is designed through a dynamic extension of the system, using the same IDA approach.

Because the resulting controller needs the derivatives of the reference currents, high-gain observers [24] are used for their calculation. The proposed controller allows obtaining a good performance

DOI: 10.1002/cta

tracking control of the compensating currents, thus ensuring an almost sinusoidal source current, with total harmonic distortion within the standards limits [25], even when the system parameters are different from those considered in the controller. This allows considering practical cases when parameter errors or variations may occur due to temperature or other external disturbances. Simulation results using a realistic converter model, which considers power converter switching and losses, grid distortion, and parameter variations, are presented in order to validate the behavior of the proposed control strategy.

2. SHUNT ACTIVE POWER FILTER MODEL

The system considered in this work consists of a power source (electric grid) feeding a nonlinear load through a transmission line. Apart from that, a SAPF is connected in parallel with the load. This filter is used to cancel the harmonic currents consumed by the load, as can be observed in Figure 1.

The nonlinear load under consideration consists of an inductive impedance (L_{ac}) connected in series to a controlled bridge rectifier (with conduction angle $\alpha = 30^{\circ}$), which feeds an inductive-resistive load (R_c, L_c), and a three-phase resistance (R_{ac}) connected in parallel to the nonlinear load, as can be observed in Figure 2.

The power converter used to implement the SAPF is a VSC, constructed with isolated gate bipolar transistors, ($S_1 \ldots S_6$), as can be observed in Figure 3.

To connect the converter to the power system in parallel, an inductive filter becomes necessary to make the VSC work as a controlled current source, allowing the injection of the compensation current into the power system.

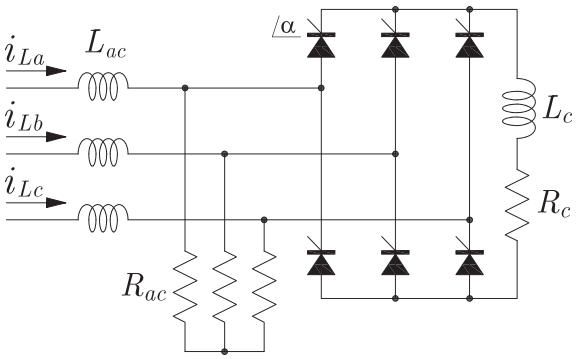

Figure 2. Nonlinear load.

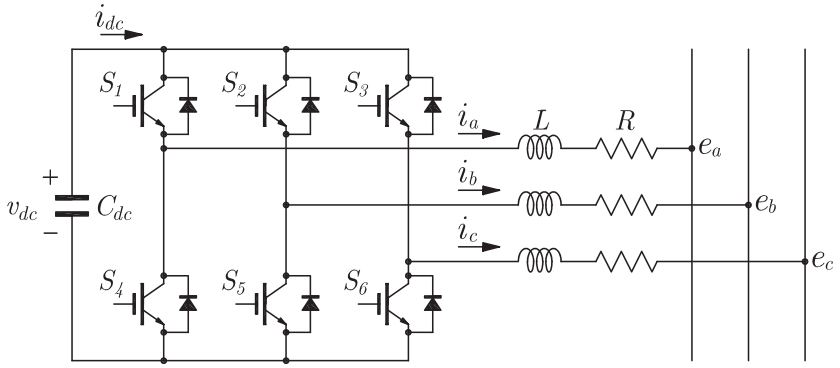

Figure 3. Power converter.

DOI: 10.1002/cta

2.1. Port Hamiltonian model of the shunt active power filter

The port-Hamiltonian (pH) systems are determined by an internal interconnection structure, a Hamiltonian defined as the total energy of the system and a resistive structure, which represents energy dissipation. Thus, they are well suited to design passivity-based control strategies through modifying the energy function and adding dissipation, e.g., through interconnection and damping assignment [17,22].

The pH model of a dynamic system can be written as,

$$\dot{\mathbf{x}} = [\mathbf{J}(\mathbf{x}) - \mathbf{R}(\mathbf{x})] \frac{\partial H(\mathbf{x})}{\partial \mathbf{x}} + \mathbf{g}(\mathbf{x})\mathbf{u} + \zeta, \tag{1}$$

where $\mathbf{x}$ is the state vector, $\mathbf{u}$ is the input vector, $\mathbf{J}(\mathbf{x}) = -\mathbf{J}^T(\mathbf{x})$ is the antisymmetrical interconnection matrix, $\mathbf{R}(\mathbf{x}) = \mathbf{R}(\mathbf{x})^T \geq 0$ is the symmetric and positive semi-definite damping matrix, $H(\mathbf{x})$ is the energy function of the system, $\mathbf{g}(\mathbf{x})$ is the input matrix, and ζ are external port signals.

The pH model of the SAPF can be expressed as follows [23]:

$$\begin{bmatrix} L\dot{i}_d \\ L\dot{i}_q \\ C_{dc}\dot{v}_{dc} \end{bmatrix} = \begin{bmatrix} -R & -\omega_{dq}L & 0 \\ \omega_{dq}L & -R & 0 \\ 0 & 0 & 0 \end{bmatrix} \begin{bmatrix} i_d \\ i_q \\ v_{dc} \end{bmatrix} + \begin{bmatrix} v_{dc} & 0 \\ 0 & v_{dc} \\ -i_d & -i_q \end{bmatrix} \begin{bmatrix} m_d \\ m_q \end{bmatrix} + \begin{bmatrix} -e_d \\ -e_q \\ 0 \end{bmatrix}, \tag{2}$$

where ω_{dq} is the angular speed of the dq reference frame, which is considered equal to the grid frequency, i_d and i_q are currents in the selected reference frame, obtained from the transformation of i_a, i_b, and i_c; e_d and e_q are the grid voltages obtained from the transformation of e_a, e_b, and e_c; v_{dc} is the DC link voltage; m_d and m_q are the modulation indices; and L and R are inductance and resistance of the filter, respectively.

The system energy $H(\mathbf{x})$ is the sum of the energy stored in the inductors of the output filter and in the DC link capacitor,

$$H(\mathbf{x}) = \frac{Li_d^2}{2} + \frac{Li_q^2}{2} + \frac{C_{dc}v_{dc}^2}{2}. \tag{3}$$

3. CONTROLLER DESIGN

The design of the controller must ensure that the state variables of the system (1) follow the trajectory defined by the reference vector,

$$\mathbf{x}^* = \begin{bmatrix} Li_d^* & Li_q^* & C_{dc}v_{dc}^* \end{bmatrix}^T, \tag{4}$$

while ensuring that tracking error ($\varepsilon = \mathbf{x} - \mathbf{x}^*$) converges to zero.

In this paper, it is proposed to design a control law $\mathbf{u}$ such that the desired closed-loop system can be described by a pH system with a new Hamiltonian $H_d(\mathbf{x}, \mathbf{x}^*)$, as follows [22],

$$\dot{\varepsilon} = [\mathbf{J}_d(\varepsilon) - \mathbf{R}_d(\varepsilon)] \frac{\partial H_d(\mathbf{x}, \mathbf{x}^*)}{\partial \varepsilon}, \tag{5}$$

with a stable equilibrium at $\varepsilon = 0$.

In this pH system, $\mathbf{J}_d(\varepsilon) = -\mathbf{J}_d^T(\varepsilon) = \mathbf{J} + \mathbf{J}_a(\varepsilon)$ and $\mathbf{R}_d(\varepsilon) = \mathbf{R}_d^T(\varepsilon) = \mathbf{R} + \mathbf{R}_a(\varepsilon) \geq 0$ are the desired interconnection and damping matrices, respectively, while $\mathbf{J}_a(\varepsilon)$ and $\mathbf{R}_a(\varepsilon)$ are the matrices used to synthesize the tracking control strategy.

DOI: 10.1002/cta

To ensure the asymptotic stability, $H_d(\mathbf{x}, \mathbf{x}^*)$ is chosen as a Lyapunov function,

$$H_d(\mathbf{x}, \mathbf{x}^*) = \frac{1}{2}\left(\varepsilon^T \mathbf{P}^{-1} \varepsilon\right), \qquad \Rightarrow \qquad H_d(\mathbf{x}, \mathbf{x}^*) = -\varepsilon^T \mathbf{P}^{-1} \mathbf{R}_d(\varepsilon) \mathbf{P}^{-1} \varepsilon < 0, \tag{6}$$

and

$$\mathbf{P} = \begin{bmatrix} L & 0 & 0 \\ 0 & L & 0 \\ 0 & 0 & C_{dc} \end{bmatrix}. \tag{7}$$

Then, $\mathbf{R}_d(\varepsilon)$ must be a positive definite matrix in order to guarantee convergence to zero of the tracking error, whose dynamic is represented by (5).

The elements of matrix $\mathbf{J}_a(\varepsilon)$ are selected in order to eliminate coupling between i_d and i_q currents, thus modifying the system's interconnection, while the elements of $\mathbf{R}_a(\varepsilon)$ are adjusted to obtain the desired convergence rate, thus,

$$\mathbf{J}_a = \begin{bmatrix} 0 & \omega_{dq} L & 0 \\ -\omega_{dq} L & 0 & 0 \\ 0 & 0 & 0 \end{bmatrix}, \mathbf{R}_a = \begin{bmatrix} R_1 & 0 & 0 \\ 0 & R_2 & 0 \\ 0 & 0 & R_3 \end{bmatrix}. \tag{8}$$

With this approach, and using (1) and (5), the following tracking matching equation can be obtained [22],

$$[\mathbf{J} - \mathbf{R}] \frac{\partial H_a(\mathbf{x}, \mathbf{x}^*)}{\partial \varepsilon} + [\mathbf{J}_a - \mathbf{R}_a] \frac{\partial H_d(\mathbf{x}, \mathbf{x}^*)}{\partial \varepsilon} - \zeta + \dot{\mathbf{x}}^* = \mathbf{g}(\mathbf{x})\mathbf{u}, \tag{9}$$

with

$$H_a(\mathbf{x}, \mathbf{x}^*) = H_d(\mathbf{x}, \mathbf{x}^*) - H(\mathbf{x}). \tag{10}$$

The solution of (9) gives the control laws for m_d and m_q,

$$m_d = \frac{1}{v_{dc}} \left[L\dot{i}_d^* + R i_d^* + \omega_{dq} L i_q - R_1 \left(i_d - i_d^*\right) + e_d\right], \tag{11}$$

$$m_q = \frac{1}{v_{dc}} \left[L\dot{i}_q^* + R i_q^* - \omega_{dq} L i_d - R_2 \left(i_q - i_q^*\right) + e_q\right]. \tag{12}$$

As can be noted from (9), control laws (11, 12) include derivatives of the desired reference trajectories. This allows a faster tracking of such references, when compared with the control laws commonly obtained for controlling power converters in other applications (e.g., [20,26]). In the SAPF case, this is necessary for a correct control of the compensating currents, as will be seen in the simulation results. Because the waveform of these references is time-varying and depends on the load characteristics, their derivatives must be calculated on-line. For this reason, in this paper, derivatives of the current references are obtained using a second-order high-gain observer [24].

With the proposed control laws, tracking error dynamics are obtained from (5) as follows:

$$\dot{\varepsilon}_{i_d} = -\frac{(R + R_1)}{L} \varepsilon_{i_d}, \tag{13}$$

DOI: 10.1002/cta

$$\dot{\varepsilon}_{i_q} = -\frac{(R+R_2)}{L}\varepsilon_{i_q}, \tag{14}$$

$$\dot{\varepsilon}_{v_{dc}} = -\frac{R_3}{C_{dc}}\varepsilon_{v_{dc}}. \tag{15}$$

Thus, R_1, R_2, and R_3 can be calculated to achieve the desired convergence speed in each variable.

The reference currents i_d^* and i_q^* are chosen so that the current supplied by the grid is sinusoidal and balanced. Such reference currents consist of the compensation currents, $i_{d_{\text{Comp}}}^*$ and $i_{q_{\text{Comp}}}^*$, necessary to fulfill the control objective, plus a current, $i_{d_{\text{Loss}}}^*$, to compensate additional losses in the system, that is,

$$i_d^* = i_{d_{\text{Comp}}}^* + i_{d_{\text{Loss}}}^*, \qquad \text{and,} \qquad i_q^* = i_{q_{\text{Comp}}}^*. \tag{16}$$

The compensation currents, $i_{d_{\text{Comp}}}^*$ and $i_{q_{\text{Comp}}}^*$, are obtained through applying the *pq* theory [23],

$$\begin{bmatrix} i_{d_{\text{Comp}}}^* \\ i_{q_{\text{Comp}}}^* \end{bmatrix} = \frac{1}{\left(e_d^{+1}\right)^2 + \left(e_q^{+1}\right)^2} \begin{bmatrix} e_d^{+1} & e_q^{+1} \\ e_q^{+1} & -e_d^{+1} \end{bmatrix} \begin{bmatrix} p_{\text{Comp}}^* \\ q_{\text{Comp}}^* \end{bmatrix}, \tag{17}$$

where

$$p_{\text{Comp}}^* = \widetilde{p}_L^{+1} \ , \qquad \text{and,} \qquad q_{\text{Comp}}^* = \overline{q}_L^{+1} + \widetilde{q}_L^{+1} = q_L^{+1} \ . \tag{18}$$

p_{Comp}^* and q_{Comp}^* are the power references, $\widetilde{p}$ and $\widetilde{q}$ represent real and imaginary oscillatory powers, and $\overline{q}$ is the constant value of imaginary power. The supra-index $^{+1}$ indicates that the power values $\widetilde{p}_L^{+1}$, $\widetilde{q}_L^{+1}$, and $\overline{q}_L^{+1}$ are calculated using the fundamental component of positive sequence voltage, e^{+1}, whereas the subindex $_L$ indicates that these values are calculated using the current consumed by load.

The current component used for compensating the additional losses (self-discharge of the DC link capacitor, switching, and conduction losses, etc.) can be obtained through balancing power in the converter and considering the dynamics of the DC link voltage. Therefore, it is possible to obtain an approximate reference for the loss current,

$$i_{d_{\text{Loss}}}^* = \frac{1}{2}\left[-\frac{e_d}{R} \pm \sqrt{\left(\frac{e_d}{R}\right)^2 - 4\left[i_q^{*2} - \frac{v_{dc}R_3}{R}\left(v_{dc} - v_{dc}^*\right)\right]}\right]. \tag{19}$$

Such reference current is obtained assuming that the current control loops are much faster than the voltage control loop ($i_d = i_d^*$ e $i_q = i_q^*$) and $e_q = 0$. Even when $i_{d_{\text{Loss}}}^*$ is obtained using an ideal model of the system (e.g., inverter losses are not included), a correct selection of R_3 allows regulating the DC link voltage to its reference value.

DC link voltage reference, v_{dc}^*, is a chosen constant so that voltage v_{dc} stays at such values that allow the converter to inject the required compensation current.

Figure 4 shows the control scheme proposed for the SAPF. This control scheme uses a PSD in order to determine e^{+1}. The PSD used in this work is a Double Second Order Generalized Integrator-Frequency Locked Loop (DSOGI-FLL) type, which presents advantages with respect to other methods regarding this particular application [27].

DOI: 10.1002/cta

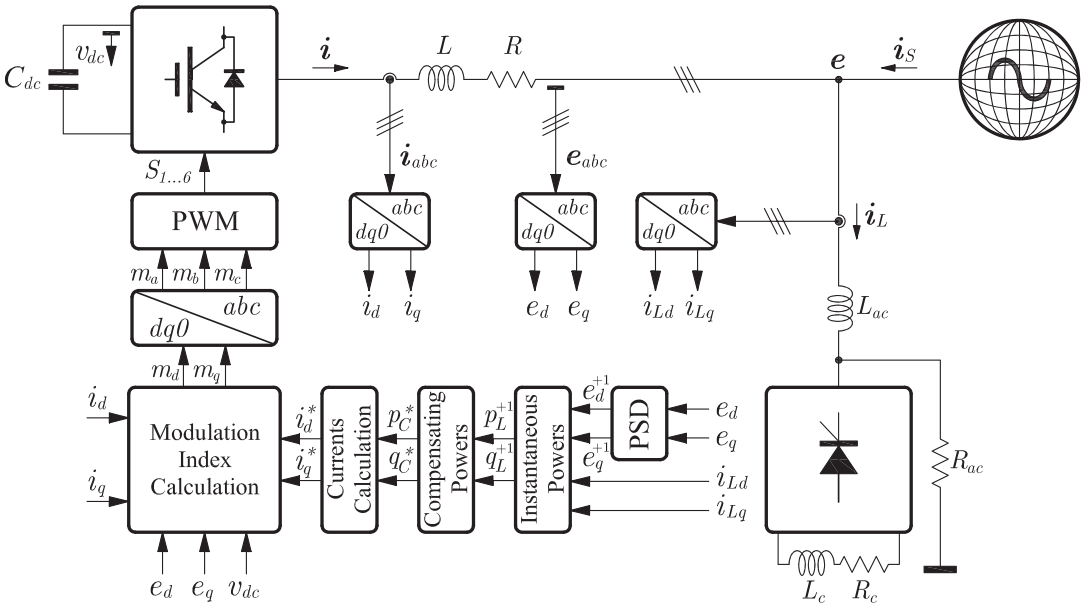

Figure 4. Proposed control strategy.

3.1. Integral action

The control laws (11) and (12) are dependent on the parameters of the system. Therefore, a steady-state error in the state variables may appear due to parameter variation. To cope with this problem, an integral action is added to the proposed controller, by extending the system as suggested in [18].

The pH model of the system with the output equation can be written as,

$$\dot{\mathbf{x}} = [\mathbf{J}(\mathbf{x}) - \mathbf{R}(\mathbf{x})] \frac{\partial H(\mathbf{x})}{\partial \mathbf{x}} + \mathbf{g}(\mathbf{x})\mathbf{u} + \zeta, \tag{20}$$

$$\mathbf{y} = \mathbf{g}^T(\mathbf{x}) \frac{\partial H(\mathbf{x})}{\partial \mathbf{x}}. \tag{21}$$

The pH model of the integral controller is

$$\dot{\varphi} = \mathbf{u}_{ca}, \tag{22}$$

$$\mathbf{y}_{ca} = \mathbf{g}^T(\varphi) \frac{\partial H_{ca}(\varphi)}{\partial \varphi} = \frac{\partial H_{ca}(\varphi)}{\partial \varphi}, \tag{23}$$

where φ is the state variable, $\mathbf{u}_{ca}$ is the input vector, $\mathbf{y}_{ca}$ is the output vector, and $H_{ca}(\varphi) = 1/2\varphi^T\varphi$ is the energy function of the integral controller.

Interconnecting this controller with the closed-loop system through negative feedback,

$$\mathbf{u}_{ca} = \dot{\varphi} = \mathbf{y} = \mathbf{g}^T(\mathbf{x}) \frac{\partial H_d(\mathbf{x}, \mathbf{x}^*)}{\partial \varepsilon}. \tag{24}$$

The energy function of the closed-loop system with the integral controller is

$$H_T(\mathbf{x}, \mathbf{x}^*, \varphi) = H_d(\mathbf{x}, \mathbf{x}^*) + H_{ca}(\varphi). \tag{25}$$

DOI: 10.1002/cta

Thus, the closed-loop system with the additional controller is a pH system of the form

$$\begin{bmatrix} \dot{\mathbf{x}} \\ \dot{\varphi} \end{bmatrix} = \begin{bmatrix} [\mathbf{J}_d(\varepsilon) - \mathbf{R}_d(\varepsilon)] & -\mathbf{g}(\mathbf{x}) \\ \mathbf{g}^T(\mathbf{x}) & 0 \end{bmatrix} \begin{bmatrix} \dfrac{\partial H_T(\mathbf{x}, \mathbf{x}^*, \varphi)}{\partial \varepsilon} \\ \dfrac{\partial H_T(\mathbf{x}, \mathbf{x}^*, \varphi)}{\partial \varphi} \end{bmatrix} + \begin{bmatrix} \dot{\mathbf{x}}^* \\ 0 \end{bmatrix}. \tag{26}$$

Solving (26), the new control laws are obtained,

$$m_d = \frac{1}{v_{dc}} \left[L\dot{i}_d^* + Ri_d^* + \omega_{dq} L i_q - R_1 \left(i_d - i_d^* \right) + e_d \right] - \varphi_d, \tag{27}$$

$$m_q = \frac{1}{v_{dc}} \left[L\dot{i}_q^* + Ri_q^* - \omega_{dq} L i_d - R_2 \left(i_q - i_q^* \right) + e_q \right] - \varphi_q, \tag{28}$$

where

$$\varphi_d = \int v_{dc} \left(i_d - i_d^* \right) dt + \int i_d \left(v_{dc} - v_{dc}^* \right) dt, \tag{29}$$

$$\varphi_q = \int v_{dc} \left(i_q - i_q^* \right) dt + \int i_q \left(v_{dc} - v_{dc}^* \right) dt. \tag{30}$$

In this way, the added integral action allows eliminating the errors produced by parameter mismatch and other disturbances, while the implemented method allows preserving the stability properties of the IDA design.

4. SIMULATION RESULTS

With the objective of evaluating the behavior of the SAPF using the control strategy proposed in the present work, two tests were designed and simulated using a real model of the system, which includes losses in the converter and switching effects. Simulations were carried out using the SimPowerSystems package of Matlab™.

The controller parameters used in the simulations are: $R_1 = R_2 = 15$ and $R_3 = 0.2$. The specifications of the SAPF and the grid are: $v_{dc} = 900\ V$, $R_{on_{(IGBT)}} = 1\ m\Omega$, $R = 1\ m\Omega$, $L = 1.5\ mH$, $C = 1000\ uF$, $f_s = 10\ kHz$, $f = 50\ Hz$, and $e_a, e_b, e_c = 311\ V$.

4.1. Balanced grid voltage

For this case, a three-phase sinusoidal and balanced voltage is assumed.

Figure 5 shows the current of phase a at different points of the system. The test starts with the system without compensation and at $t = 0.05$s; the SAPF is connected to compensate the harmonic currents consumed by the load.

Figure 5(a and b) shows the waveforms of the compensation current (i_a) and the current supplied by the source (i_{Sa}), respectively, for the same test. As can be appreciated in Figure 5(a), compensating currents have sharp slopes. This highlights the need of an accurate tracking control of such currents, which can be obtained thanks to the proposed control laws that include derivatives of the reference currents.

If the classic IDA design were used, similar control laws would be obtained but without including derivatives of the reference currents. This case is included for comparison purposes in Figure 6 (a and b). As can be seen, in this case, the SAPF is not able to completely compensate the nonlinear load effects, thus resulting in a supply current, which is not completely sinusoidal.

In order to verify that the current consumed from the grid is sinusoidal and balanced using the proposed strategy, a Fourier spectral decomposition was carried out based on the analysis of

DOI: 10.1002/cta

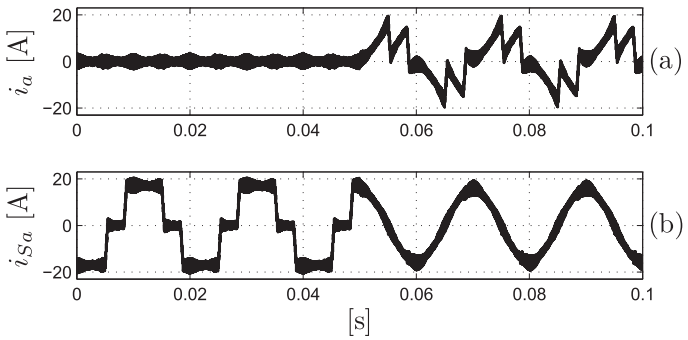

Figure 5. Currents of phase *a* of the system (balanced grid voltage). (a) compensating current and (b) source current.

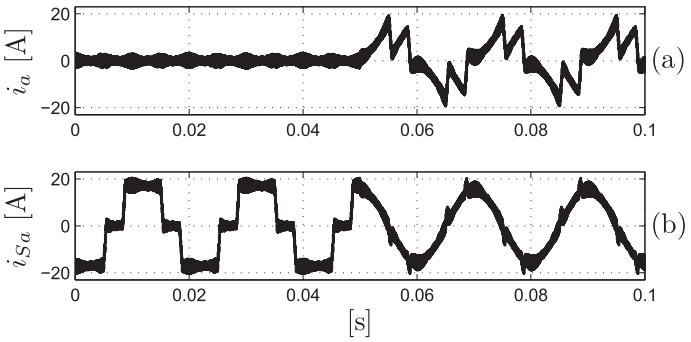

Figure 6. Currents of phase *a* of the system (balanced grid voltage) with classic interconnection and damping assignment design. (a) compensating current and (b) source current.

sequence components, that is, positive values (blue) mean positive sequence harmonics, while negative values (red) are used to represent negative sequence harmonics. Figure 7(a) shows the spectrum of i_{Sa} current for $t < 0.05$s (without compensation) and Figure 7(b) shows the spectrum for $t \geq 0.05$s (with compensation). It can be observed that components corresponding to the 7th, 13th, and 19th harmonics, which are characteristic of this type of nonlinear load, reduce noticeably ($< 1\,\%$) using the proposed SAPF controller. Again, for comparison with the classic IDA design, Figure 7(c) includes the spectrum of the source current shown in Figure 6(b). As can be appreciated, even when in this case harmonics are compensated, their value cannot be maintained below $1\,\%$, for the same controller adjustment.

For this test, total harmonic distortion (THD) of the current consumed from the grid is 26.89% without compensation, while the maximum THD value is 5% according to standards. After applying the compensation using the proposed controller, THD of such currents is reduced to 1.86%, while using the controller designed with the classic IDA methodology, THD results 7.87%. As it can be clearly seen, controller design using modified IDA technique allows reducing the currents THD to values accepted by standards.

Figure 8 shows the DC link voltage and its reference value. As can be observed in this figure, the proposed control strategy allows regulating v_{dc}, while tying it to its reference value from the instant, the SAPF starts working. It can also be observed that the ripple that appears in voltage at 0.05s stays within admissible limits.

If there are differences between the system parameters and those considered in the control, a distortion in the current consumed from the grid appears, even using the proposed tracking control. Figure 9(a and b) shows the waveform of i_a and its frequency spectrum, respectively, for a test where variations of $50\,\%$ in the inductance and resistance of the connection filter are considered.

In the frequency spectrum of Figure 9(b), it is observed that the values of harmonics components amplitude are higher than those shown in Figure 7(b) because of the error in the L and R values

DOI: 10.1002/cta

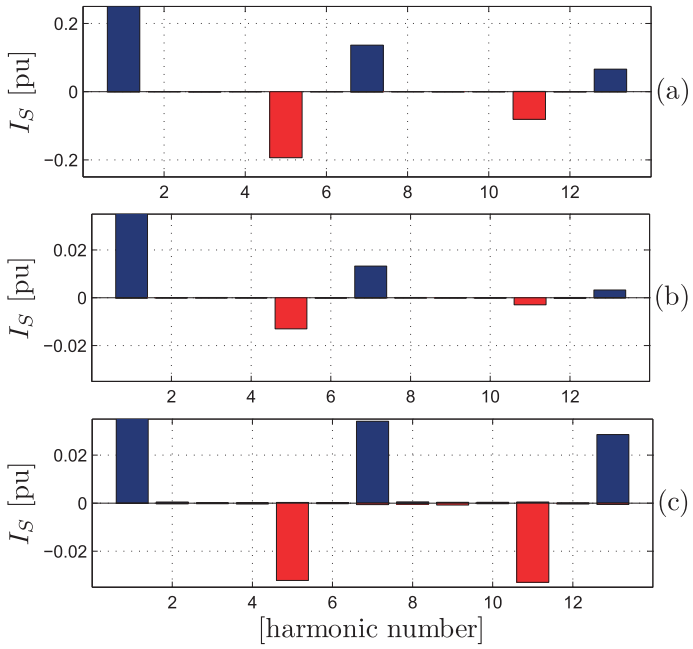

Figure 7. Frequency spectrum of the source current (balanced grid voltage). (a) without compensation; (b) with compensation; and (c) with compensation with the classic interconnection and damping assignment design.

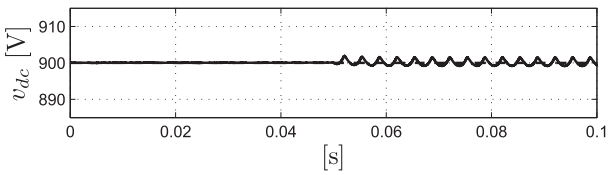

Figure 8. Direct current link voltage for the balanced grid voltage test.

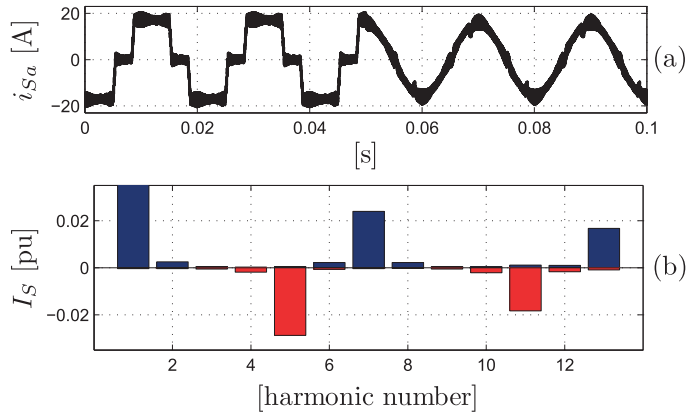

Figure 9. Current of phase a of the system for parameter variations without integral controller. (a) source current and (b) frequency spectrum of the source current with compensation.

used in the controller. The THD of the source current in this case results 5.2 %, thus exceeding the allowable values for the standards.

With the aim of solving this problem, the controller with integral action (27) and (28) is used. Figure 10(a) shows the waveform of i_a and Figure 10(b) the corresponding frequency spectrum.

DOI: 10.1002/cta

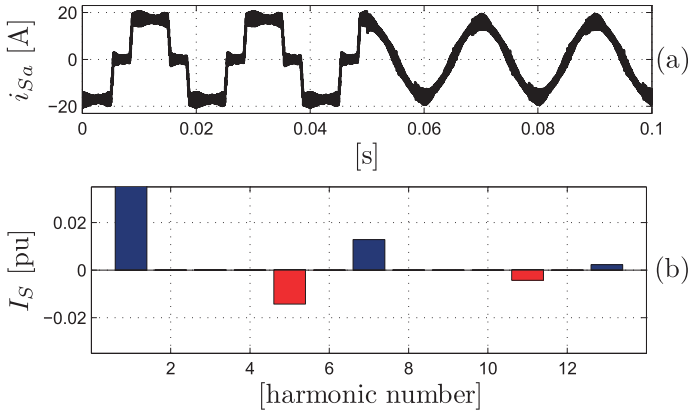

Figure 10. Current of phase a of the system for parameter variations with integral controller. (a) source current and (b) frequency spectrum of the source current with compensation.

As observed in Figure 10(b), the harmonic components are significantly reduced, and THD is now 1.91 %.

4.2. *Grid voltage with unbalance and harmonics*

A three-phase grid voltage with 13 % unbalance according to the International Electrotechnical Commission standard and 5 % 5th harmonic plus 2 % 7th harmonic is used for this test.

Figure 11 shows current in phase a, before and after the filter is connected. Figure 11(a and b) shows waveforms of the compensation current (i_a) and of the current supplied by the source (i_{Sa}), respectively, for the same test.

Figure 12(a) shows the current spectrum for $t < 0.05$s (no compensation), and Figure 12(b) shows the current spectrum for $t \geq 0.05$s (compensation).

Because of unbalance and to the harmonics components of the grid voltage, low-amplitude negative sequence components and additional harmonics ($\pm$ 3rd, + 5th, − 7th, $\pm$ 9th, etc.) appear in the spectrum.

Using the proposed filter, the harmonics components are attenuated so as to obtain amplitudes below 1 %. THD of the currents consumed from the grid results 3.33% in this case, which is a value accepted by standards.

Figure 13 shows voltage on the DC link and its reference value. It can be observed that the proposed control strategy allows regulating v_{dc} and that the ripple that appears at the instant the SAPF is connected stays within admissible limits.

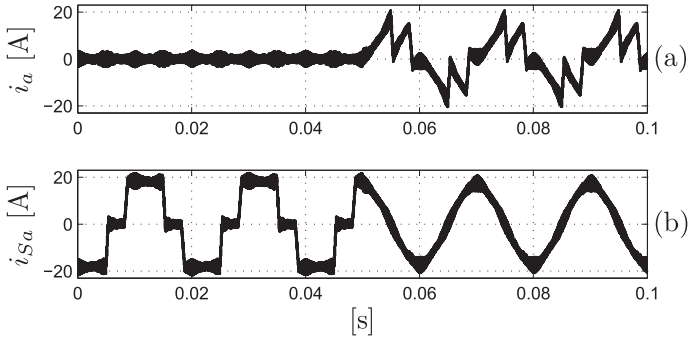

Figure 11. Currents in phase a of the system (grid voltage with unbalance + harmonics). (a) compensating current and (b) source current.

DOI: 10.1002/cta

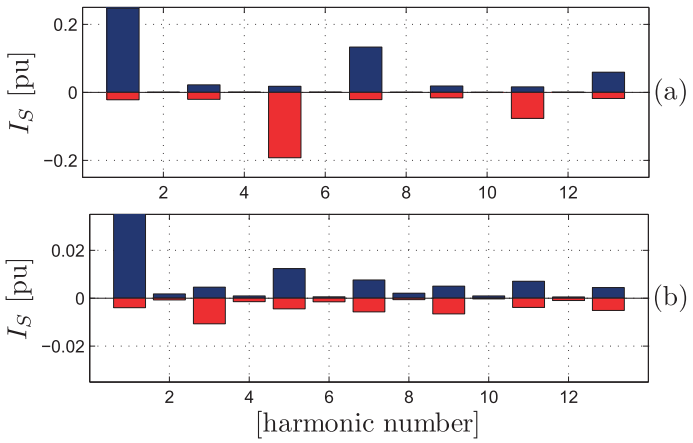

Figure 12. Frequency spectrum of the source current (grid voltage with unbalance + harmonics). (a) without compensation and (b) with compensation.

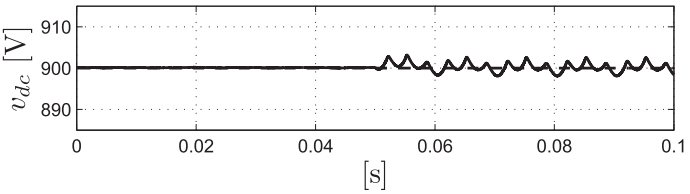

Figure 13. Direct current link voltage for grid voltage with unbalance and harmonics.

5. CONCLUSIONS

A control strategy designed using the IDA technique for a SAPF was proposed in the present work, with the main objective of compensating the harmonics currents consumed by nonlinear load, while making the current supplied by the source be sinusoidal and balanced. The *pq* theory was used to determine the reference values of the compensation currents to be synthesized by the converter.

The design was made using an IDA technique modified to allow solving a tracking control problem. The modified IDA design guarantees convergence to zero of the tracking error. This design implies including derivatives of the current references in the control laws, which allows improving the control of compensating currents when compared with the classic IDA design, thus resulting in a better cancelation of the load harmonics. Because compensating currents depend on the load and their waveforms can be time-varying, high-gain observers were used to obtain the derivatives of the reference currents. Besides, an integral action was added to the proposed controller in order to eliminate the errors produced by parameter uncertainties.

Two simulation tests were carried out, one of them for sinusoidal and balanced grid voltages, and the other for grid voltages with unbalance and harmonics. In the first test, results show that the proposed strategy allows reducing the harmonics introduced by the nonlinear load, maintaining them below 1 %, as stated in the standards. It is also shown that the use of the modified IDA strategy allows a better compensation of the load current harmonics, when compared with the classic IDA design, for the same controller parameters.

Furthermore, errors due to parameters variation are eliminated by adding integral action to modified IDA controller.

The second test showed that, besides the harmonic currents characteristic of nonlinear load, those harmonics introduced by distortions on the source voltage can be reduced noticeably by using the SAPF with the proposed control strategy.

DOI: 10.1002/cta

ACKNOWLEDGEMENTS

This work was supported by the Universidad Nacional de San Luis, by the Universidad Nacional de Río Cuarto, by the FONCyT-ANPCyT, and by the Consejo Nacional de Investigaciones Científicas y Técnicas (CONICET).

REFERENCES

1. Akagi H, Watanabe EH, Aredes M. *Instantaneous Power Theory and Applications to Power Conditioning*. John Wiley & Sons, Inc.: Hoboken, New Jersey, 2007.
2. Kale M, Ozdemir E. An adaptive hysteresis band current controller for shunt active power filter. *Electric Power Systems Research* 2005; **73**(2):113–119.
3. Xu L, Han Y, Khan MM, Pan J-M, Chen C, Yao G, Zhou L-D. Analysis and effective controller design for the cascaded H-bridge multilevel APF with adaptive signal processing algorithms. *Int. Journal of Circuit Theory and Applications* 2011; **40**(7):635–659.
4. Ramos-Carranza H, Medina A. Optimization-based method for shunt hybrid filter compensation in non-stiff systems. *Int. Journal of Circuit Theory and Applications* 2013; **41**(5):457–482.
5. Green TC, Marks JH. Control techniques for active power filters. *IEE Proceedings Electric Power Applications* 2005; **152**(2):369–381.
6. Lo Y-K, Pan T-F, Wang J-M. On setting the DC voltage level of an active power filter, *Int. Journal of Circuit Theory and Applications* 2008; **36**(8): 975–982.
7. Abdusalam M, Poure P, Karimi S, Saadate S. New digital reference current generation for shunt active power filter under distorted voltage conditions. *Electric Power Systems Research* 2009; **79**(5):759–765.
8. Akagi H, Kanazawa Y, *Nabae A*. Generalized theory of the instantaneous reactive power in three-phase circuits, *JIEE IPEC* 1983: 1375–1386.
9. Zhong Q, Zhang Y, Yang J, Wu J. Non-linear auto-disturbance rejection control of parallel active power filters. *IET Control Theory & Applications* 2009; **3**(7):907–916.
10. Ortega R, Loría A, Nicklasson P, Sira-Ramírez H. *Passivity-Based Control of Euler–Lagrange Systems. Mechanical, Electrical and Electromechanical Applications*. Springer-Verlag: London, 1998.
11. Doria-Cerezo A, Batlle C, Espinosa-Perez G. Passivity-based control of a wound-rotor synchronous motor. *IET Control Theory & Applications* 2010; **4**(10):2049–2057.
12. Shiau L-G, Lin J-L, Yeh Y-J. Passivity based control for induction motor drives with voltage-fed and current-fed inverters. *Electric Power Systems Research* 2001; **59**(1):1–11.
13. Batlle C, Dòria-Cerezo A, Ortega R. Power flow control of a doubly-fed induction machine coupled to a flywheel. *European Journal of Control* 2005; **11**(3):209–221.
14. Espinosa-Pérez G, Maya-Ortiz P, Dòria-Cerezo A, Moreno J. Output-feedback IDA Stabilization of a SMIB system using a TCSC. *International Journal of Control* 2010; **83**(12):2471–2482.
15. Mancilla-David F, Ortega R. Adaptive passivity-based control for maximum power extraction of stand-alone windmill systems. *Control Engineering Practice* 2012; **20**(2):173–181.
16. Batlle C, Dòria-Cerezo A. Bidirectional power flow control of a power converter using passive Hamiltonian techniques. *Int. Journal of Circuit Theory and Applications* 2008; **36**(7):769–788.
17. Ortega R, van der Schaft A, Maschke B, Escobar G. Interconnection and damping assignment passivity-based control of port-controlled Hamiltonian systems. *Automatica* 2002; **38**(4):585–596.
18. Ortega R, Garcia-Canseco E. Interconnection and damping assignment passivity-based control: a survey. *European Journal of Control* 2004; **10**:432–450.
19. Gaviria C, Fossas E, Grino R. Robust controller for a full-bridge rectifier using the IDA approach and GSSA modeling. *IEEE Transactions on Circuits and Systems* 2005; **52**(3):609–616.
20. Serra FM, De Angelo CH, Forchetti DG. IDA-PBC control of a three-phase front-End converter, *38th Annual Conference on IEEE Industrial Electronics Society*, *IECON* 2012; 5203–5208.
21. Escobar G, Chevreau D, Ortega R, Mendes E. An adaptive passivity-based controller for a unity power factor rectifier. *IEEE Transactions on Control Systems Technology* 2001; **9**(7):637–644.
22. Wang Z, Goldsmith P. Modified energy-balancing-based control for the tracking problem. *IET Control Theory & Applications* 2008; **2**(4):310–322.
23. Serra FM, De Angelo CH, Forchetti DG. IDA-PBC control of shunt active filters for harmonics compensation, *Sixth IEEE/PES Transmission and Distribution*: *Latin America Conference and Exposition*, *T&D-LA*, 2012; 1–6.
24. Dabroom A, Khalil HK. Numerical differentiation using high-gain observers, *IEEE 36th Conference on Decision and Control*, 1997; 4790–4795.
25. IEEE recommended practices and requirements for harmonic control in electrical power systems, *IEEE Std* 519–1992, 1993.
26. Tang Y, Yu H, Zou Z. Hamiltonian modeling and energy-shaping control of three-phase ac/dc voltage-source converters, *IEEE Int. Conf. on Automation and Logistics*, *ICAL*, 2008; 591–595.
27. Serra FM, Forchetti DG, De Angelo CH. Comparison of positive sequence detectors for shunt active filter control, *IEEE Int. Conf. on Industry Applications*, *INDUSCON*, 2010, 1–6.

DOI: 10.1002/cta